GeoVirtual 2020 September 14-16 Resilience and Innovation

Analytical Solutions for Dynamic Consolidation of Soft Clay Ground under Different Loading Modes

Shuangxi Feng, Huayang Lei & Yongfeng Wan
Department of Civil Engineering-Tianjin University, Tianjin, China
Chen Lin
Department of Civil Engineering – University of Victoria, Victoria, BC, Canada

ABSTRACT
The analytical solutions of single-layered ground consolidation were studied under the sinusoidal loading, triangular loading and rectangular loading mode. The series separation variable method (SSVM) was applied to the solution. Research shows that the settlement of ground caused by sinusoidal loading is the largest, followed by rectangular loading and triangular loading. The finite element method was adapted, DLOAD subroutines of different loading modes were programmed in FORTRAN language, and the differences between analytical and numerical solutions were compared and analyzed. Furthermore, the refraction law of elastic stress wave and SSVM were employed to solve the analytical solution. The influence of modulus ratio on dynamic consolidation deformation of double-layered ground was discussed. Results demonstrated that the larger the modulus ratio of double-layered ground is, the larger the soil deformation presents.

RÉSUMÉ
Les solutions analytiques de consolidation de sol monocouche ont été étudiées sous le chargement sinusoïdal, le chargement triangulaire et le mode de chargement rectangulaire. La méthode des variables de séparation en série (SSVM) a été appliquée à la solution. La recherche montre que le tassement du sol causé par la charge sinusoïdale est le plus important, suivi par la charge rectangulaire et la charge triangulaire. La méthode des éléments finis a été adaptée, des sous-programmes DLOAD de différents modes de chargement ont été programmés en langage FORTRAN, et les différences entre les solutions analytiques et numériques ont été comparées et analysées. En outre, la loi de réfraction de l'onde de contrainte élastique et de la SSVM a été utilisée pour résoudre la solution analytique. L'influence du rapport de module sur la déformation de consolidation dynamique du sol à double couche a été discutée. Les résultats ont démontré que plus le rapport de module du sol à double couche est élevé, plus la déformation du sol est importante.

1 INTRODCTION

With the rapid development of China's economic construction, a large number of infrastructure construction is booming in coastal cities, where the soft clay is widely distributed. However, the dynamic consolidation problem is prominent for soft clay ground. The consolidation of soft clay leads to the drainage of water in the soil under the complex traffic loading, and the soft clay ground may produce an excessive settlement. The dynamic consolidation belongs to the fluid-solid coupling, however, the majority of the literature reviews focuses on the consolidation of soft clay under static loadings rather than dynamic loadings. In engineering practice, the soft ground in coastal areas is subject to a complex traffic loading. Definitely, sinusoidal loading, triangular loading and rectangular loading are often used to simulate traffic loading modes, and the amplitude of traffic loading is about 50kPa~100kPa (Cai et al. 2012; Mohanty and Ranjan. 2014; Lei et al. 2019). However, the different loading modes have a great influence on the dynamic consolidation deformation characteristics of soil. Therefore, it is critical and necessary to explore the deformation development of soft clay ground under different dynamic loading modes.

Terzaghi (1925) established consolidation theory and gave the corresponding analytical solution to predict the consolidation in single-layered soil under the static loading. Analytical solutions for dynamic consolidation of single-layered soft clay ground have been an interesting topic and an increasing number of theoretical studies on it can be found in Duncan (1993), Wang et al. (2003) and Chen (2004). Wilson et al. (1974) and Baligh et al. (1978) respectively developed an analytical solution for the consolidation of a soil layer subjected to a cyclic square loading. Alonso et al. (1974) studied a random loading solution for consolidation. Wu et al. (1994) offered the solution under arbitrary cyclic loading using the Laplace transform method. Although many studies show the

analytical solution of consolidation, it often needs to solve complex partial differential equations, which brings a lot of inconvenience to calculation analysis and engineering application. New methods provide a guarantee for dynamic consolidation such as Laplace transform and matrix transformation method, numerical analysis. Cai et al. (1998) used the Laplace transform and matrix transformation method to solve the one-dimensional consolidation of soft clay ground under the complex conditions of nonlinear, viscoelastic, variable load and stress history. A numerical method of differential quadrature method (DQM) for solving partial differential equations is proposed by Mittal et al. (2011), the main idea is solving algebraic equations after DQM transformation.

Layered soil consolidation calculation problems are often encountered in engineering practice, and layered soil consolidation theory has always been concerned. Gray (1945) first established a linear consolidation model of double-layered soil and gave its analytical solution under a constant loading. Xie et al. (1999) presented a fully explicit analytical solution for the consolidation of partially drained boundaries double-layered soil subjected to constant loading. Davis and Raymond (1965) obtained a nonlinear consolidation solution for homogeneous soils by assuming that the compressibility of the soil during compaction is proportional to the change in permeability. The linearity and nonlinearity of the saturated soft clay ground under different boundary conditions are widely investigated. For example, nonlinear consolidation behavior was analyzed and solved numerically by Liu et al. (2009), Xie et al. (2007) and Ejian et al.(2009), who used Hansbo formula and the non-Darcy flows considering the initial water flow gradient.

Although many scholars are devoted to the analytical solution of dynamic consolidation deformation of soft clay ground, there is no consensus in theoretical analysis. Especially on the simplification of dynamic loading, different scholars regard dynamic traffic loading as sinusoidal loading, triangular loading and rectangular loading according to research problems. However, few experts have carried out systematic research on the consolidation deformation of single or double-layered soft clay ground under three loading modes of sinusoidal loading, triangular loading and rectangular loading. Therefore, based on Terzaghi's consolidation theory, the analytical solution of dynamic consolidation deformation of the single-layered ground under three loading modes is obtained by using the method of series separation of variables. Using ABAQUS finite element software, DLOAD subroutines of different loading modes are implemented by FORTRAN language, and the differences of analytical and numerical solutions of dynamic consolidation deformation of soft clay ground under different loading stress amplitudes are compared and analyzed. At the same time, the refraction law of elastic stress wave and the method of series separation variable are used to solve the analytical solution of dynamic consolidation deformation of double-layered soft clay ground, and the influence of modulus ratio on dynamic consolidation deformation of the double-layered ground is discussed.

2 PROBLEM DESCRIPTION AND BASIC ASSUMPTIONS

Terzaghi (1925) proposed the consolidation theory of saturated clay soil. The mathematical derivations are based on the following six assumptions (Taylor, 1948).

1. The clay-water system is homogeneous.
2. Saturation is complete.
3. Compressibility of water is negligible.
4. Compressibility of soil grains is negligible.
5. The flow of water is in the direction of compression.
6. Darcy's law is valid.

According to the Terzaghi's consolidation theory, the model calculation diagram is established in Figure 1. If the soil is completely saturated, the soil particles and pore water are incompressible, the volume change of the soil element should be equal to the difference between the surface flow and the volume, where depth is z, the height is dz in the soil element. Hence, the volume of compression, ΔV, is shown in Eq. 1.

$$\Delta V = m_v \frac{\partial \sigma'}{\partial t} dzdt \quad [1]$$

where, σ' is defined as an effective stress, t is time, m_v is equal to the ratio between compressibility coefficient α and initial void ratio e_0 plus 1, $m_v=\alpha/(1+ e_0)$.

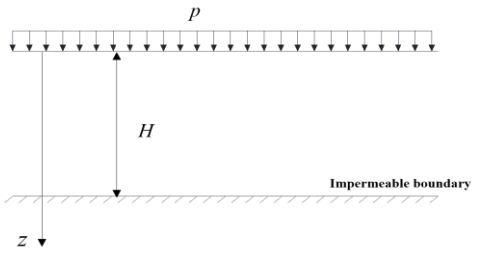

Figure. 1 Model calculation diagram

On the basis of the effective stress principle, effective stress σ' is followed by Eq. 2:

$$\sigma' = \sigma - u = p + \gamma' H - u \quad [2]$$

where σ is the total stress, u is the pore water pressure, p is the loading pressure, H is the depth of ground, γ' is the effective unit weight.

Combined Eq. 1 with Eq. 2, thus

$$\Delta V = m_v (\frac{\partial p}{\partial t} + \gamma' \frac{\partial H}{\partial t} - \frac{\partial u}{\partial t}) A dzdt \quad [3]$$

where A is the hexahedron unit area

Continuous deformation condition demonstrates that $\Delta V = \Delta Q$. Thus,

$$\Delta Q = -\frac{\partial q}{\partial z} dzdA = -\frac{1}{\gamma_w} \frac{\partial}{\partial z} (k \frac{\partial u}{\partial z}) A dzdt \quad [4]$$

where q is the water discharge per time, γ' is the water unit weight, k is the hydraulic conductivity.

So, the general form of one-dimensional consolidation equation is followed by Eq. 5:

$$(\frac{\partial^2 u}{\partial z^2} + \frac{1}{k} \frac{\partial k}{\partial z} \frac{\partial u}{\partial z}) + \frac{1}{C_v} (\frac{\partial p}{\partial t} + \gamma' \frac{\partial H}{\partial t} - \frac{\partial u}{\partial t}) = 0 \quad [5]$$

where C_v is the consolidation coefficient.

Three loading modes shown in Figure 2 are considered in this paper, i.e. sinusoidal loading, triangular loading and rectangular loading. The expression of the three loadings in initial one cycle is as follows:

Sinusoidal loading: $p = \sigma_d \sin(wt + \varphi) \quad (t_1 \le t \le t_2)$ [6]

Triangular loading: $p = \begin{cases} c_1 t \quad (0 \le t \le t_1) \\ c_1 t_1 - c_1 \quad (t_1 < t \le t_2) \end{cases}$ [7]

Rectangular loading: $p = \begin{cases} c_2 (0 \le t \le t_1) \\ 0 (t_1 < t \le t_2) \end{cases}$ [8]

where, σ_d is the amplitude of sinusoidal load, w is circular frequency, φ is the initial phase angle, c_1 is the slope of the loading line, c_2 is the amplitude of rectangular loading. t_1 and t_2 are the start and end time in a single cycle.

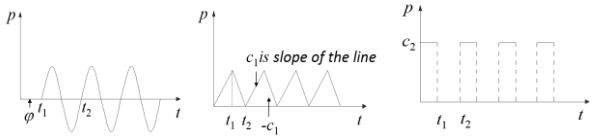

(a) Sinusoidal loading (b) Triangular loading (c) Rectangular loading

Figure 2 Three loading modes

3 ANALYTICAL SOLUTIONS FOR DYNAMIC CONSOLIDATION OF THE SINGLE-LAYERED GROUND

3.1 Single-layered ground under the sinusoidal loading

The constant of α_v, e, H, k and the variable of p is assumed, according to the Eq. 5, we can obtain the Eq. 9.

$$\frac{\partial^2 u}{\partial z^2} + \frac{1}{C_v}\left(\frac{\partial p}{\partial t} - \frac{\partial u}{\partial t}\right) = 0 \quad [9]$$

The partial differential equation 10 is given based on the Eq. 9

$$\frac{\partial u}{\partial t} = C_v \frac{\partial^2 u}{\partial z^2} + wA\cos(wt + \varphi) \quad [10]$$

Boundary conditions are as follows:

$$\begin{cases} u(z,0) = u_0 \\ u(0,t) = 0 \\ \dfrac{\partial u}{\partial z}\Big|_{z=H} = 0 \end{cases} \quad [11]$$

where u_0 is initial pore water pressure.

Series separation variable method is applied to the partial differential equation 10. There are two steps to get the solution of the equation: first, find the solution of the homogeneous equation, which can determine the intrinsic function system and the form of solution. And then, the form of solution is determined by boundary condition 11.

The form of solution of homogeneous equation is as follows:

$$u(z,t) = X(z)T(t) \quad [12]$$

where, X(Z) and T(t) are the function of depth and time.

Combined the Eq. 12 with the partial differential equation 10, Eq. 13 can be obtained as follows:

$$X(z)T'(t) = C_V X''(z)T(t) \quad [13]$$

$$\frac{T'(t)}{C_V T(t)} = \frac{X''(z)}{X(z)} = -\lambda \quad [14]$$

where, λ is the scale parameter

$$T'(t) + \lambda C_v T(t) = 0 \quad [15]$$

$$\begin{cases} X''(z) + \lambda X(z) = 0 \\ X(0) = 0, X'(H) = 0 \end{cases} \quad [16]$$

When λ>0, Eq. 16 has the nonzero solution. Thus

$$X(z) = A\cos\sqrt{\lambda}z + B\sin\sqrt{\lambda}z \quad [17]$$

where, A and B are the control parameter

Because $X(0) = 0$, $A = 0$. Hence, $X(x) = B\sin\sqrt{\lambda}x$, $X'(H) = 0$. Thus

$$\sqrt{\lambda}B\cos\sqrt{\lambda}H = 0 \quad [18]$$

Because $\sqrt{\lambda}B \ne 0$, $\cos\sqrt{\lambda}H = 0$, $\sqrt{\lambda} = \dfrac{n\pi - \dfrac{\pi}{2}}{H}$ and $\lambda_n = \left(\dfrac{n\pi - \dfrac{\pi}{2}}{H}\right)^2 \quad n = 1,2,...$

Intrinsic function system is as follows:

$$\left\{\sin\left(\frac{(2n-1)\pi}{2H}z\right)\right\} \quad [19]$$

Hence, the solution of partial differential equation is assumed by Eq. 20:

$$u(z,t) = \sum_{n=0}^{\infty} T_n(t)\sin\left(\frac{(2n-1)}{2H}\pi z\right) \quad [20]$$

where $u_t = \sum_{n=0}^{\infty} T_n(t)\sin\left[\dfrac{(2n-1)}{2H}\right]$,

$$u_{zz} = -\sum_{n=0}^{\infty} T_n(t) \bullet \sin\left(\frac{(2n-1)}{2H}\pi z\right) \bullet \left(\frac{(2n-1)}{2H}\pi\right)^2$$

Combined with Eq. 10, the Eq. 21 is established.

$$\sum_{n=0}^{\infty}\left[T'_n(t) + \left(\frac{(2n-1)}{2H}\pi\sqrt{C_v}\right)^2 T_n(t)\right]\sin\frac{2n-1}{2H}\pi z = \sum_{n=0}^{\infty} f_n \sin\frac{(2n-1)}{2H}\pi z \quad [21]$$

where f_n is in accordance with the Fourier transformation, thus

$$f_n = \frac{2}{H}\int_0^H wA\cos(wt+\varphi)\sin\frac{(2n-1)}{2H}\pi z dz = \frac{4wA\cos(wt+\varphi)}{(2n-1)\pi} \quad [22]$$

$$\begin{cases} T'_n(t) + \left(\dfrac{(2n-1)}{2H}\pi\sqrt{C_v}\right)^2 T_n(t) = \dfrac{4wA\cos(wt+\varphi)}{(2n-1)\pi} \\ T_n(0) = u_0 \end{cases} \quad [23]$$

According to the general solution of $y' + p(x)y = q(x)$, $y = e^{-\int p(x)dx}\left[C + \int q(x)e^{-\int p(x)dx}dx\right]$. Thus,

$$T_n(t) = e^{-\int\left(\frac{2n-1}{2H}\pi\sqrt{C_v}\right)^2 dt} \bullet \left[C + \int \frac{4wA\cos(wt+\varphi)}{(2n-1)\pi} e^{\int\left(\frac{(2n-1)}{2H}\pi\sqrt{C_v}\right)^2 dt} dt\right] \quad [24]$$

$$T_n(t) = e^{-\frac{(2n-1)^2}{4H^2}\pi C_v t}\left[C + \frac{4wA}{(2n-1)} \bullet \frac{w\sin(wt+\varphi)e^{\frac{(2n-1)^2\pi^2 C_v t}{4H^2}} + e^{\frac{(2n-1)^2}{4H^2}\pi^2 C_v t}\cos(wt+\varphi)}{1+w^2}\right] \quad [25]$$

The constant of C is obtained by the boundary conditions.

$$T(0)=u_0=1+\left(C+\frac{4wA}{(2n-1)\pi}\bullet\frac{w\sin\varphi+\cos\varphi}{1+w^2}\right) \quad [26]$$

$$C=u_0-1-\frac{4wA}{(2n-1)\pi}\bullet\frac{w\sin\varphi+\cos\varphi}{1+w^2} \quad [27]$$

$$T_n(t)=e^{-\frac{(2n-1)^2}{4H^2}\pi C_v t}\left[(u_0-1-\frac{4wA(w\sin\varphi+\cos\varphi)}{(2n-1)\pi(1+w^2)})+\frac{4wAe^{\frac{(2n-1)^2\pi^2C_vt}{4H^2}}(w\sin(wt+\varphi)+\cos(wt+\varphi))}{(2n-1)(1+w^2)}\right] \quad [28]$$

Thus, the analytical solutions of partial differential equation 29 in single cycle:

$$\begin{aligned}u_i(z,t)&=\sum_{n=0}^{\infty}T_n\bullet\sin(\frac{2n-1}{2H})\pi z\\&=\sum_{n=0}^{\infty}e^{\frac{(2n-1)^2}{4H^2}\pi C_v t}\left[(u_0-1-\frac{4wA(w\sin\varphi+\cos\varphi)}{(2n-1)\pi(1+w^2)})+\frac{4wAe^{\frac{(2n-1)^2\pi^2C_vt}{4H^2}}(w\sin(wt+\varphi)+\cos(wt+\varphi))}{(2n-1)(1+w^2)}\right]\\&\bullet\sin(\frac{2n-1}{2H})\pi z\end{aligned} \quad [29]$$

3.2 Single-layered ground under the triangular loading and rectangular loading

Combined Eq. 9 with boundary condition 11, the nonlinear partial differential equation 30 for dynamic consolidation of soft clay ground under the triangular loading is established as follows:

$$\begin{cases}u_t=C_Vu_{zz}+C_1\\u(0,t)=0,u_z\big|_{z=H}=0\\u(z,0)=u_0\end{cases}\text{(a) or }\begin{cases}u_t=C_Vu_{zz}-C_1\\u(0,t)=0,u_z\big|_{z=H}=0\\u(z,0)=u_0\end{cases}\text{(b)} \quad [30]$$

Similarly, the intrinsic function system of homogeneous partial differential equation is shown in Eq. 31

$$\left\{\sin\left(\frac{(2n-1)\pi}{2H}z\right)\right\} \quad [31]$$

So the solution of the non-line partial differential equation can be set as follows:

$$u(z,t)=\sum_{n=0}^{\infty}T_n(t)\sin(\frac{(2n-1)}{2H}\pi z) \quad [32]$$

Eq. 32 is substituted into the Eq. [30,a], we can get Eq. 33:

$$\sum_{n=0}^{\infty}\left[T_n^{'}(t)+(\frac{(2n-1)}{2H}\pi\sqrt{C_v})^2T_n(t)\right]\sin\frac{2n-1}{2H}\pi z=\sum_{n=0}^{\infty}f_n\sin\frac{(2n-1)}{2H}\pi z \quad [33]$$

f_n is expanded in accordance with the Fourier series, thus

$$f_n=\frac{2}{H}\int_0^H C_1\sin\frac{(2n-1)}{2H}\pi z dz=\frac{2C_1}{(2n-1)\pi} \quad [34]$$

$$\begin{cases}T_n^{'}(t)+(\frac{(2n-1)\pi}{2H}\sqrt{C_v})^2T_n(t)=\frac{2C_1}{(2n-1)\pi}\\T_n(0)=u_0\end{cases} \quad [35]$$

$$T_n(t)=e^{-\int\left(\frac{(2n-1)\pi}{2H}\sqrt{C_v}\right)^2dt}\bullet\left[C+\int\frac{2C_1}{(2n-1)\pi}e^{-\int\left(\frac{(2n-1)\pi}{2H}\sqrt{C_v}\right)^2dt}dt\right] \quad [36]$$

$$=e^{-\frac{(2n-1)^2\pi^2}{4H^2}C_vt}\bullet\left[C-\frac{8C_1H^2}{(2n-1)^3\pi^3}e^{-\frac{(2n-1)^2\pi^2}{4H^2}C_vt}\right]$$

$T_n(0)=u_0=C-\frac{8C_1H^2}{(2n-1)^3\pi^3}$, $C=u_0+\frac{8C_1H^2}{(2n-1)^3\pi^3}$ is obtained as follows:

$$T_n(t)=e^{-\frac{(2n-1)^2\pi^2}{4H^2}C_vt}\bullet\left[(u_0+\frac{8C_1H^2}{(2n-1)^3\pi^3})-\frac{8C_1H^2}{(2n-1)^3\pi^3}e^{-\frac{(2n-1)^2\pi^2}{4H^2}C_vt}\right] \quad [37]$$

$$u_i(z,t)=\sum_{n=0}^{\infty}e^{-\frac{(2n-1)^2\pi^2}{4H^2}C_vt}\bullet\left[u_0+\frac{8C_1H^2}{(2n-1)^3\pi^3}\left(1-e^{-\frac{(2n-1)^2\pi^2}{4H^2}C_vt}\right)\right]\bullet\sin\frac{(2n-1)}{2H}\pi z \quad [38]$$

Based on Eq. 9 and boundary condition 11, the nonlinear partial differential equation 39 for one-dimensional dynamic consolidation of soft clay ground subjected to triangular loading is also established as follows:

$$\begin{cases}u_t=C_Vu_{zz}\\u(0,t)=0,u_z\big|_{z=H}=0\\u(z,0)=u_0\end{cases} \quad [39]$$

The problem is simplified as a one-dimensional consolidation theory. So the analytical solution is as follows:

$$u(z,t)=\frac{4p}{\pi^2}\sum_{n=0}^{\infty}\frac{1}{n^2}\left(n\pi\alpha+2(-1)^{\frac{n-1}{2}}(1-\alpha)\right)e^{-\frac{n^2\pi^2}{4}T_V}\bullet\sin\frac{n\pi z}{2H} \quad [40]$$

To describe the variation of accumulative pore water pressure, the pore water pressure of each cycle is added up, as shown in Eq. 41.

$$u_{T_i}(z,t)=\sum_{1}^{i-1}u_{T_i}(z,t) \quad [41]$$

Combined with the definition of consolidation degree, the settlement prediction formula of soft clay ground can be determined, as shown in Eq.42.

$$s_t=U\bullet s_\infty=(1-\frac{u_{Ti}(z,t)}{\sigma})\bullet s_\infty \quad [42]$$

Combined with the results of analytical solution, the load amplitude of 50kPa, 80kPa and 100kPa respectively is selected based on the result proposed by Tang et al. (2009), which can simulate the traffic loading. The vibration frequency is 2Hz, the consolidation time is 30 days, the hydraulic conductivity is 0.0035m/d, the elastic modulus of soft clay ground is 3.854MPa, and the void ratio is 1.5.

Figure 3 shows that the surface settlement increases with time and presents the fluctuation, which is different from the settlement development under the static loading. For the sinusoidal and triangular loadings, the settlement development form is basically consistent with the loading mode, which is different from the rectangular loading. This is mainly due to the soft clay ground is in the consolidation state during the process of rectangular loading. The settlement of soft clay ground under constant loading shows a rapid growth trend. When the loading is equal to 0 kPa, the soft clay ground still has consolidation under the gravity load. When the load is suddenly applied, the excess pore water pressure rises suddenly, the effective stress decreases, and the settlement rebounds, which is the main reason why there is no rectangular repeated vibration.

In addition, the settlement increases with the increase of loading amplitude. When the amplitude is 50kPa, 80kPa and 100kPa, the corresponding settlement is respectively 16.76mm, 26.81mm and 33.51mm for sinusoidal loading, 8.44mm, 13.50mm and 16.88mm for triangular loading, 8.96mm, 14.34mm and 17.92mm for rectangular loading. Obviously, the dynamic deformation of soft clay caused by sinusoidal loading is larger than that caused by rectangular loading. And the dynamic deformation of soft clay caused by triangular loading is the smallest. Therefore, the influence of different loading modes on the dynamic consolidation deformation of soft clay ground should be emphasized in engineering practice.

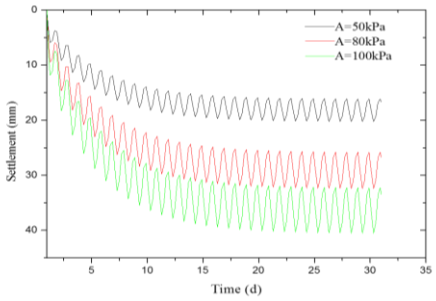

(a) Sinusoidal loading

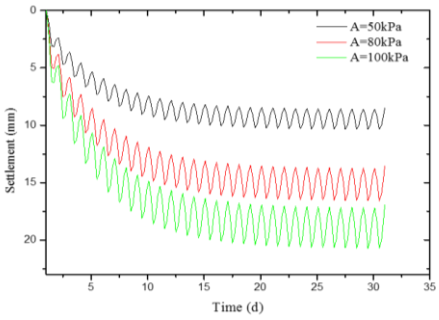

(b)Triangular loading

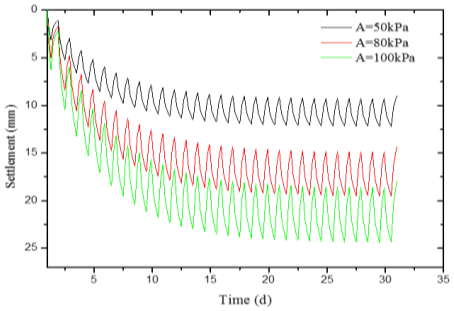

(c) Rectangular loading

Figure 3 Settlement curve of soft clay ground under different loading amplitudes

To illustrate the correctness of the analytical solution of dynamic consolidation deformation of single-layered soft clay ground under different loading modes, the results of the finite element are compared and verified. The boundary condition of the finite element is the key to the solution and iterative convergence. It needs to satisfy the boundary conditions of force, displacement and initial stress field. Force boundary condition: apply body force to form the in-situ stress field, set three different loading modes at the X_{max} position of the ground surface. Different loading modes need to be implemented through DLOAD subroutines programmed in FORTRAN language.

Displacement boundary condition: fixed constraint is adopted for X_{min} at the bottom of the model, horizontal displacement constraint is set at the position of Y_{min} and Y_{max} of the model, and pore water pressure is set to zero at X_{max} of the ground surface, namely, the ground surface can drain freely. The model size is 10 m × 20 m, adopting the structured grid separation technology, 200 units are divided, and fluid-solid coupling element is chosen, as shown in Figure 4

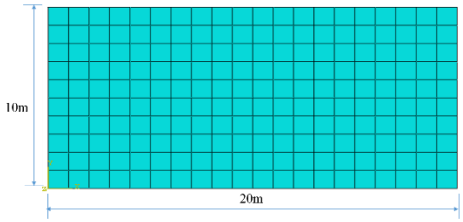

Figure 4 Finite element analysis model of single- layered soft clay ground

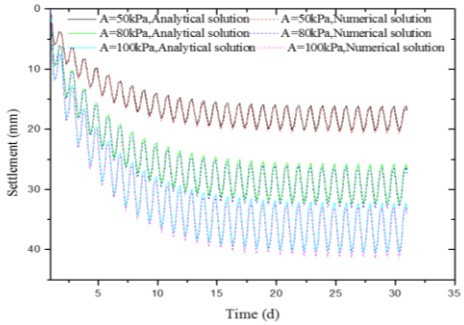

(a) Sinusoidal loading

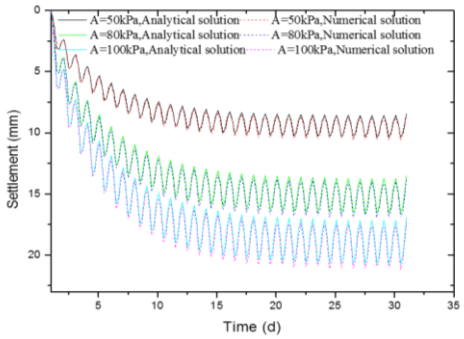

(b)Triangular loading

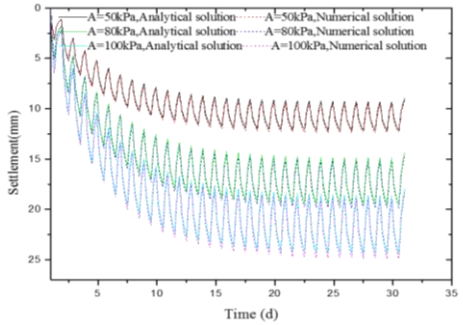

(c) Rectangular loading

Figure 5 Comparison of analytical and numerical solutions of soft clay deformation under different loading modes

Figure 5 shows that the numerical solution is basically consistent with the analytical solution. Through the statistical analysis, the maximum relative error between the numerical solution and the analytical solution of sinusoidal loading is approximately 1.2%, which can prove the correctness of the analytical solution of the deformation of single-layered soft clay ground.

4 ANALYTICAL SOLUTIONS FOR ONE-DIMENSIONAL DYNAMIC CONSOLIDATION OF THE DOUBLE-LAYERED GROUND

The consolidation problem of the layered ground is often encountered in the engineering practice. But Terzaghi's consolidation theory cannot be applied directly. To solve the problem, the bisector double-layered ground within the depth of 10m is chosen as an example, the concept of energy loss is proposed, which can solve the problem of double-layered ground and can be transformed into single-layered ground. In addition, the influence of different modulus ratios of the upper and lower layers of soft clay ground on the dynamic consolidation deformation are investigated.

In terms of layered elastic media, when the elastic shear wave propagates to the interface of two layers of soil, the wave will occur wave reflection and refraction, as shown in Figure 6. Considering that shear waves can cause a large settlement of the ground, this paper only considers the deformation of soil caused by shear waves.

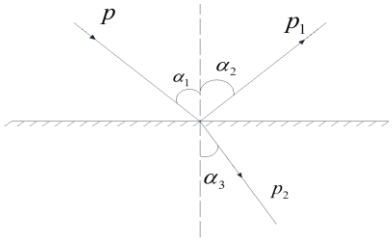

Figure 6 reflection and refraction of wave in layered interface

Eq. 43 is given by the reflection and refraction law, as follows:

$$\alpha_1 = \alpha_2 \quad [43\text{-a}]$$

$$\frac{\sin\alpha_1}{v_1} = \frac{\sin\alpha_3}{v_2} \quad [43\text{-b}]$$

where, α_1, α_2 and α_3 are angle of incidence, the angle of reflection and the angle of refraction. v_1 and v_2 are, respectively, the upper and lower layers of the shear wave velocity. The shear wave velocity, v_1 and v_2 can be expressed by $v_1 = \sqrt{\frac{G_1}{\rho_1}}$ and $v_2 = \sqrt{\frac{G_2}{\rho_2}}$. ρ_1 and ρ_2 are the upper and lower layers of the density.

The calculation of the stress wave is considered in the calculation process of the double-layered ground. When the elastic shear wave propagates to the interface of two layers of soil, the wave is refracted and reflected. According to the kinetic energy theorem, the degree of energy loss is defined as Eq. 44.

$$\delta = \frac{\frac{1}{2}\rho_1 v_1^2 - \frac{1}{2}(\rho_2+\rho_1)v_2^2}{\frac{1}{2}\rho_1 v_1^2} = \frac{G_1 - \frac{\rho_1}{\rho_2}G_2 - G_2}{G_1} \quad [44]$$

where, G_1 and G_2 are the initial shear modulus for upper layer and lower layer.

Taking the homogeneous ground into account, the upper-layered loading, p_1, of the ground can be transmitted to the lower-layered ground, which is the lower-layered loading p_2. So, the loading acting on the lower-layered ground can be defined as Eq. 45.

$$p_2(t) = \delta p_1(t) \quad [45]$$

Therefore, solutions of the dynamic consolidation under the sinusoidal loading, triangular loading and rectangular loading are shown in Eq. [46- 48]. The specific loading transfer principle is shown in Figure 7.

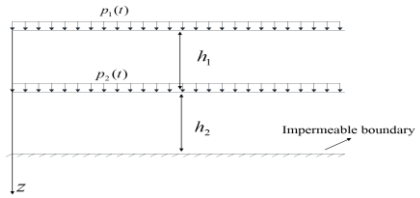

Figure 7 Dynamic consolidation calculation model of double - layered soft clay ground

$$u_1(z,t) = \sum_{n=0}^{\infty} T_n \bullet \sin(\frac{2n-1}{2H})\pi z$$
$$= \sum_{n=0}^{\infty} e^{-\frac{(2n-1)^2}{4H^2}\pi C_v t}\left[(u_0 - 1 - \frac{4wA(w\sin\varphi+\cos\varphi)}{(2n-1)\pi(1+w^2)}) + \frac{4wAe^{\frac{(2n-1)^2\pi^2 C_v t}{4H^2}}(w\sin(wt+\varphi)+\cos(wt+\varphi))}{(2n-1)(1+w^2)}\right]$$
$$\bullet \sin(\frac{2n-1}{2H})\pi z \quad [46\text{-a}]$$

$$u_2(z,t) = \sum_{n=0}^{\infty} T_n \bullet \sin(\frac{2n-1}{2H})\pi z$$
$$= \sum_{n=0}^{\infty} e^{-\frac{(2n-1)^2}{4H^2}\pi C_v t}\left[(u_0 - 1 - \frac{4wA(w\sin\varphi+\cos\varphi)}{(2n-1)\pi(1+w^2)}) + \frac{4wAe^{\frac{(2n-1)^2\pi^2 C_v t}{4H^2}}(w\delta\sin(wt+\varphi)+\cos(wt+\varphi))}{(2n-1)(1+w^2)}\right]$$
$$\bullet \sin(\frac{2n-1}{2H})\pi z \quad [46\text{-b}]$$

$$u_1(z,t) = \sum_{n=0}^{\infty} e^{-\frac{(2n-1)^2\pi^2}{4H^2}C_v t} \bullet \left[u_0 + \frac{8c_1H^2}{(2n-1)^3\pi^3}\left(1 - e^{-\frac{(2n-1)^2\pi^2}{4H^2}C_v t}\right)\right] \bullet \sin\frac{(2n-1)}{2H}\pi z \quad [47\text{-a}]$$

$$u_2(z,t) = \sum_{n=0}^{\infty} e^{-\frac{(2n-1)^2\pi^2}{4H^2}C_v t} \bullet \left[u_0 + \frac{8\delta c_1H^2}{(2n-1)^3\pi^3}\left(1 - e^{-\frac{(2n-1)^2\pi^2}{4H^2}C_v t}\right)\right] \bullet \sin\frac{(2n-1)}{2H}\pi z \quad [47\text{-b}]$$

$$u_1(z,t) = \frac{4p_2}{\pi^2}\sum_{n=0}^{\infty}\frac{1}{n^2}\left(n\pi\alpha + 2(-1)^{\frac{n-1}{2}}(1-\alpha)\right)e^{-\frac{n^2\pi^2}{4}T_V} \bullet \sin\frac{n\pi z}{2H} \quad [48\text{-a}]$$

$$u_2(z,t) = \frac{4\delta p_2}{\pi^2}\sum_{n=0}^{\infty}\frac{1}{n^2}\left(n\pi\alpha + 2(-1)^{\frac{n-1}{2}}(1-\alpha)\right)e^{-\frac{n^2\pi^2}{4}T_V} \bullet \sin\frac{n\pi z}{2H} \quad [48\text{-b}]$$

The variation of accumulative pore water pressure is also described by Eq. 49.

$$u_{1,T_i}(z,t) = \sum_{1}^{i-1} u_{T_i}(z,t)\,(a) \quad u_{2,T_i}(z,t) = \sum_{1}^{i-1} u_{T_i}(z,t)\,(b) \quad [49]$$

In light of the analytical solution of the deformation of the double-layered soft clay ground, the modulus ratio can reflect the deformation characteristics of the double-layered soft clay ground. The "upper soft and lower hard

ground" and "upper hard and lower soft ground" are the relative concepts of stratum rigidity. The thickness of both upper-layered soil and lower-layered ground is 5m, and the loading amplitude is 100kPa. The influence of the modulus ratio between upper and lower layered soil of 0.33, 0.5, 1, 2 and 4 on the analytical solution of soft clay ground deformation is analyzed.

Figure 8-10(a) illustrates that the surface settlement increases with the increase of modulus ratio. When the modulus ratio is 1, the soft clay ground is homogeneous. When the modulus ratio is 0.3 and 0.5. The soft clay ground presents "upper soft and lower hard". The relative rigidity of the lower-layered ground is large, which leads to a decrease of ground settlement. The modulus ratio is 2.0 and 4.0, and the soft clay ground shows "upper hard and lower soft". The stiffness of the lower-layer ground is relatively small, and the subsoil produces a large settlement, which eventually leads to the increase of surface settlement.

Figure 8-10 (b) shows that the settlement of lower-layered ground is inconsistent with the surface settlement of upper-layered ground. For the homogeneous ground (modulus ratio of 1.0), the settlement is the largest. This is mainly due to the reflection and refraction of the stress wave at the layered interface in the process of propagation, resulting in energy loss.

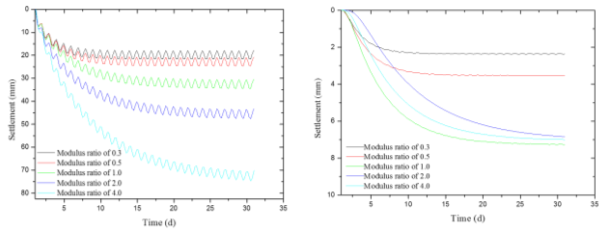

(a) Upper –layered settlement (b) Lower –layered settlement

Figure 8 Analytical solution of consolidation deformation of soft clay ground under sinusoidal loading

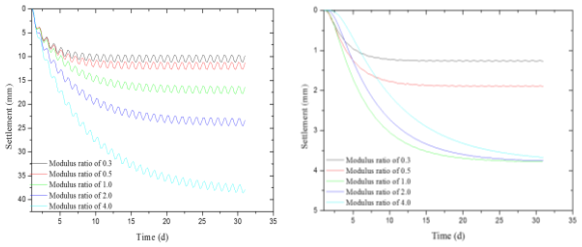

(a) Upper –layered settlement (b) Lower –layered settlement

Figure 9 Analytical solution of consolidation deformation of soft clay ground under triangular loading

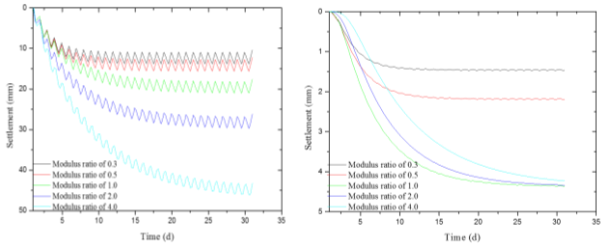

(a) Upper –layered settlement (b) Lower –layered settlement

Figure 10 Analytical solution of consolidation deformation of soft clay ground under rectangular loading

To verify the correctness of the analytical solution, the numerical solution of double-layered soft clay ground is developed. The model size, boundary condition and loading mode are consistent with the numerical solution of single-layered ground.

The difference between numerical solution and analytical solution of soft clay under sinusoidal loading, triangular loading and rectangular loading is investigated. Figure (11-13) shows that the analytical solution is in good agreement with the numerical solution under three loading modes, so the correctness of the numerical solution can be proved. Through the statistical analysis, the maximum errors of settlement caused by sinusoidal loading, triangular loading and rectangular loading are 5.26%, 4.92%, 4.76%, respectively.

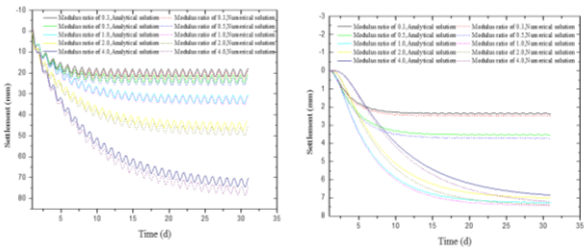

(a) Upper –layered settlement (b) Lower –layered settlement

Figure 11 Comparison of analytical and numerical solutions of ground deformation of soft clay under sinusoidal loading

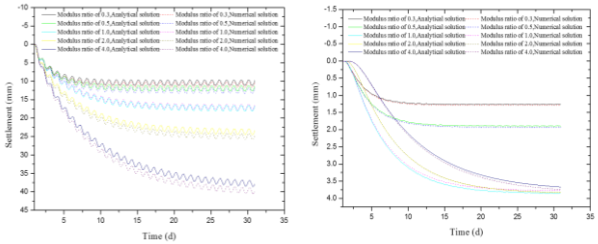

(a) Upper –layered settlement (b) Lower –layered settlement

Figure 12 Comparison of analytical and numerical solutions of ground deformation of soft clay under triangular loading

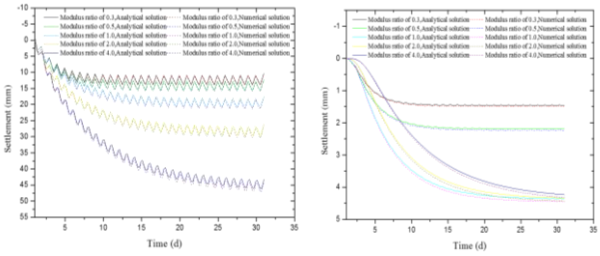

(a) Upper –layered settlement (b) Lower –layered settlement

Figure 13 Comparison of analytical and numerical solutions of ground deformation of soft clay under rectangular loading

5 CONCLUSIONS

Based on the Terzaghi's consolidation theory, the analytical solutions of single-layered and double-layered soft clay ground under three loading modes of sinusoidal loading, triangular loading and rectangular loading are obtained. The analytical solution of single-layered ground is obtained by the method of series separation of variables; the analytical solution of double-layered ground is obtained by combining the method of series separation of variables, the law of refraction of stress wave and the degree of energy loss. On this basis, the difference between the analytical solution and the numerical solution is compared and analyzed, the correctness of the analytical solution is verified, and the dynamic consolidation deformation of ground soil is discussed by the different loading magnitudes and modulus ratios, the following conclusions can be drawn:

(1) The surface settlement increases with the increase of loading amplitudes. Under the same amplitude, the settlement caused by sinusoidal loading is larger than that caused by rectangular loading and triangular loading.

(2) For the double-layered ground, the larger the modulus ratio is, the larger the deformation of the soil performs.

(3) The analytical solution of consolidation deformation of soft clay ground has good consistency with the numerical solution, which proves the correctness of the analytical solution. The maximum relative error between analytical solution and numerical solution is 1.2% in terms of the single-layered ground, is 5.26% for the double-layered ground.

6 ACKNOWLEDGMENTS

The authors acknowledge the National Key Research and Development Program of China (Grant No. 2017YFC0805402), the Open Project of State Key Laboratory of Disaster Reduction in Civil Engineering (Grant No. SLDRCE17-01), Incentive Fund for Overseas Visits of Doctoral Students of Tianjin University in 2019 (070-0903077101), China Scholarship Council (CSC. 201906250153) for their financial support.

7 REFERENCES

Alonso, E. E. and Krizek, R. J. 1974. Randomness of settlement rate under stochastic load. *Journal of Engineering Mechanics Division*, ASCE, 100(6):1211-1226.

Baligh,M. M. and Levadoux, J. N., 1978. Consolidation theory for cyclic loading. *Journal of Geotechnical Engineering Division*, ASCE, 104(4):415-421.

Cai, Y., Xu, C. and Ding, D. 1998. One-dimensional consolidation of layered and saturated soils under cyclic loading. *Chinese Journal of Vibration Engineering*, 11(2):184-193.

Cai, G., Liu, S. and Puppala, A. J. 2012. Liquefaction assessments using seismic piezocone penetration (SCPTU) test investigations in Tangshan region in China. *Soil Dynamics and Earthquake Engineering*, 41: 141-150.

Chen, Y. M., Tang, X. W. and Wang, J. 2004. An analytic solution of one-dimensional consolidation for soft sensitive soil ground. *International Journal for Numerical and Analytic Methods in Geomechanics*, 28(9): 919-930.

Davis, E. H. and Raymond, G. P. 1965. A non-linear theory of consolidation. *Géotechnique*, 15(2):161-173.

Duncan, J. M. 1993. Limitations of conventional analysis of consolidation settlement, 27th Terzaghi lecture. J*ournal of Geotechnical Engineering Division*, ASCE, 119(9): 1333-1358.

Ejian, Cheng, Gang. and Sun, A. 2009. One-dimensional consolidation of saturated cohesive soil considering non-Darcy flows. *Chinese Journal of Geotechnical Engineering*, 31(7): 1115-1119.

Gray, H. 1945. Simultaneous consolidation of contiguous layers of unlike compressible soils. *Trans.* ASCE, 110:1327-1356.

Lei, H., Feng, S., Jia, R. and Jiang, M. 2019. Experimental investigation of the deformation characteristics of Tianjin clays under coupled dynamic stress and seepage fields. *Advances in Civil Engineering*, 2019:1-13.

Liu, Z., Sun, L., Yue, J. and Ma, Z. 2009. One-dimensional consolidation theory of saturated clay based on non-Darcy flow. *Chinese Journal of Rock Mechanics and Engineering*, 28(5):974-979.

Mittal, R. C. and Jiwari, R. 2011. Numerical study of two-dimensional reaction-diffusion brusselator system by differential quadrature method. *International Journal for Computational Methods in Engineering Science and Mechanics*, 12(1): 14-25.

Mohanty, S. and Patra, N. R. 2014. Cyclic behavior and liquefaction potential of Indian pond ash located in seismic zones III and IV. *Journal of materials in civil engineering*, 26(7): 06014012.

Tang, L., Xu, T., Lin, P. and Yu, H. 2009. Study on dynamic stress characters of layered road system under traffic loading. *Chinese Journal of Rock Mechanics and Engineering*, 28(S2):3876-3884.

Taylor, D. W. 1948. Fundamentals of soil mechanics, Wiley, New York.

Terzaghi, K. 1925. Principles of soil mechanics. *Engineering News-Record*, 95(19-27): 19-32.

Wang, H. Z., Chen, Z. and Huang. Bo. 2003. Computation of one-dimensional consolidation of double layered ground using differential quadrature method. *Journal of Zhejiang University-SCIENCE A*, 4(2): 195-201.

Wilson, N. E. and Elgohary, M. M. 1974. Consolidation of soils under cyclic loading. *Canadian Geotechnical Journal*, 11(3): 420-423.

Wu, S. M. 1994. Theory of one-dimensional consolidation of double-layered ground and its application. *Chinese Journal of Geotechnical Engineering*, 16(5):24-35.

Xie, H., Wu, Q., Zhao, Z., Jin, X. and Li, J. 2007. Consolidation computation of aquitard considering non-Darcy flow. *Rock and Soil Mechanics*, 28(5):1061-1065.

Xie, K. H., Xie, X. Y. and Gao, X. 1999. Theory of one-dimensional consolidation of two layered soil with partially drained boundaries. *Computers and Geotechnics*, 24:265-278.